AGU PUBLICATIONS

Geophysical Research Letters

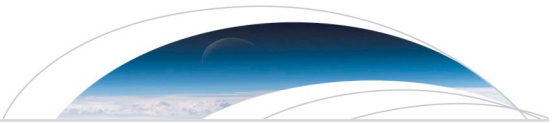

RESEARCH LETTER
10.1002/2017GL076601

Key Points:
- Topographical and hydrological controls of fast ice flow are identified in the Recovery/Slessor/Bailey Region
- We infer ancient ice flow coupling of Slessor and Recovery Glaciers through a deep, sharp gate in the bed topography
- Changes in ice sheet dynamics probably occurred and could reoccur in the Recovery/Slessor/Bailey Region

Supporting Information:
- Supporting Information S1

Correspondence to:
A. Diez,
diez@npolar.no

Citation:
Diez, A., Matsuoka, K., Ferraccioli, F., Jordan, T. A., Corr, H. F., Kohler, J., et al. (2018). Basal settings control fast ice flow in the Recovery/Slessor/Bailey Region, East Antarctica. *Geophysical Research Letters*, *45*, 2706–2715. https://doi.org/10.1002/2017GL076601

Received 30 NOV 2017
Accepted 19 FEB 2018
Accepted article online 28 FEB 2018
Published online 30 MAR 2018

Basal Settings Control Fast Ice Flow in the Recovery/Slessor/Bailey Region, East Antarctica

Anja Diez[1], Kenichi Matsuoka[1], Fausto Ferraccioli[2], Tom A. Jordan[2], Hugh F. Corr[2], Jack Kohler[1], Arne V. Olesen[3], and René Forsberg[3]

[1]Norwegian Polar Institute, Tromsø, Norway, [2]British Antarctic Survey, Cambridge, UK, [3]National Space Institute, Technical University of Denmark, Kongens Lyngby, Denmark

Abstract The region of Recovery Glacier, Slessor Glacier, and Bailey Ice Stream, East Antarctica, has remained poorly explored, despite representing the largest potential contributor to future global sea level rise on a centennial to millennial time scale. Here we use new airborne radar data to improve knowledge about the bed topography and investigate controls of fast ice flow. Recovery Glacier is underlain by an 800 km long trough. Its fast flow is controlled by subglacial water in its upstream and topography in its downstream region. Fast flow of Slessor Glacier is controlled by the presence of subglacial water on a rough crystalline bed. Past ice flow of adjacent Recovery and Slessor Glaciers was likely connected via the newly discovered Recovery-Slessor Gate. Changes in direction and speed of past fast flow likely occurred for upstream parts of Recovery Glacier and between Slessor Glacier and Bailey Ice Stream. Similar changes could also reoccur here in the future.

1. Introduction

The outlet glaciers, Recovery, Slessor, and Bailey, comprise 15% of Antarctica's grounded area (Rignot et al., 2008). These glaciers penetrate far inland from the grounding line (Mouginot et al., 2017) and drain 5% of Antarctica's fresh water outflow into the Filchner Ice Shelf (Rignot et al., 2008, 2011). Golledge et al. (2017) identified this region, part of Coats Land and Dronning Maud Land, as the most significant East Antarctic contributor to sea level rise for this century and subsequent millennia. Future enhanced ice loss from the Recovery/Slessor/Bailey Region may occur due to the penetration of warmer circumpolar deep water into the sub–Filchner Ice Shelf cavity, causing ice shelf thinning and, thus, a reduction of buttressing for the inflowing glaciers (Hellmer et al., 2012). Understanding the glaciological setting and ice stream dynamics in the region is critical to better predict the response of this vulnerable sector of the East Antarctic Ice Sheet to ocean warming and changing climate.

Controls on the location and mass flux of glaciers can range from topographic boundaries to differences in basal conditions due to sediments and/or water (Winsborrow et al., 2010). This leads to variable governing mechanisms of ice flow and ultimately variable sensitivities and response times of fast ice flow tributaries to atmospheric and oceanic forcing.

Previous work in the area investigated basal settings of Institute and Möller Ice Streams, which drain part of the West Antarctic Ice Sheet into the Filchner-Ronne Ice Shelf. Their ice flow stability is inferred to be influenced by a combination of basal sediments and water and has potentially experienced dynamical instabilities in the past (Bingham & Siegert, 2007a; Jordan et al., 2013; Rippin et al., 2014; Siegert et al., 2016). Less is known about basal conditions beneath the neighboring Recovery/Slessor/Bailey Region.

Previous studies of the Recovery/Slessor/Bailey Region are limited to the Slessor catchment and the Recovery Lakes. Fast ice flow, which we define here as ice flow of 15 m/yr and faster, originates on Recovery Glacier in the vicinity of the large subglacial Recovery Lakes A–D (labeled in Figure 1) (Bell et al., 2007). Numerous active subglacial lakes under Recovery Glacier (Fricker et al., 2014) imply that subglacial water plays a significant role in the control of ice flow here. A large subglacial basin in the Recovery catchment was inferred from surface terrain analysis (Le Brocq et al., 2008). Slessor Glacier consists of three main tributaries. The fast ice flow of the two southern tributaries was interpreted to be driven by internal deformation (Rippin et al., 2003, 2004). The fast ice flow of the northern tributary is thought to be largely driven by basal motion due to the presence

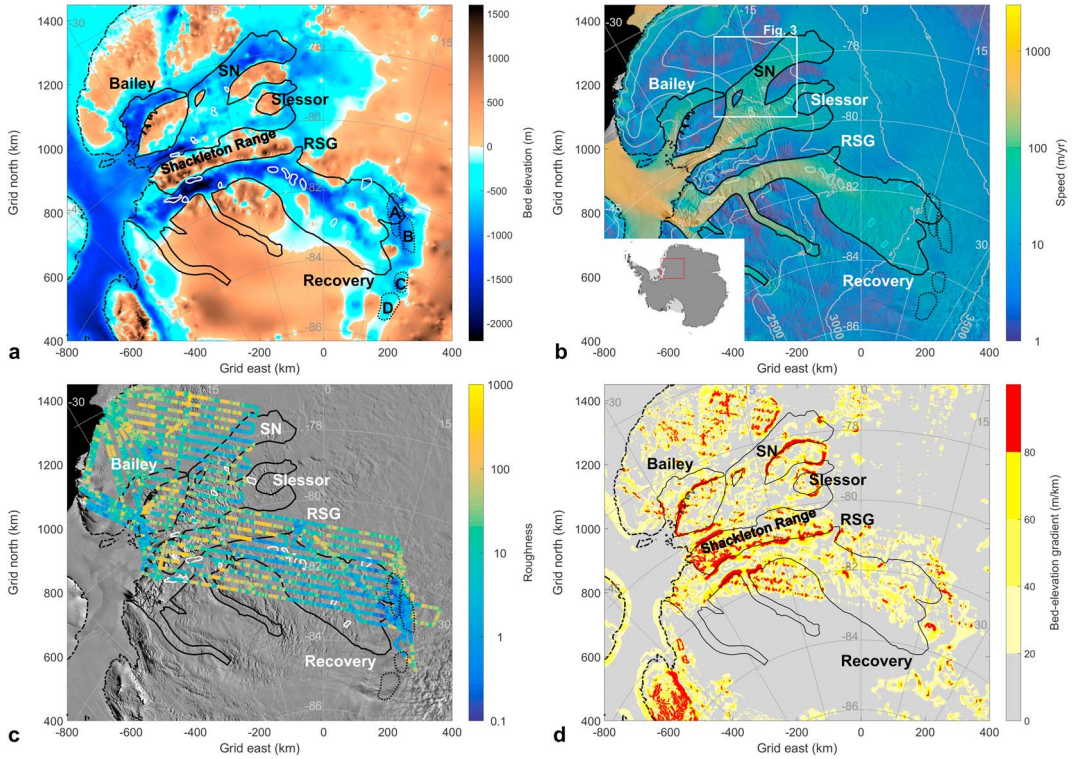

Figure 1. Bed topography (a), ice flow (b), bed roughness (c), and bed elevation gradient (d) of the Recovery/Slessor/Bailey Region, Antarctica (inset; Antarctic Polar Stereographic projection, true scale at −71°, EPSG3031). (a) New bed topography map (reference WGS84 ellipsoid) derived from new bed elevation data and existing Bedmap2 data (Figure S1) (Fretwell et al., 2013). (b and c) Plotted on Moderate Resolution Imaging Spectroradiometer (MODIS) image (Haran et al., 2014) are (b) ice flow speed (Mouginot et al., 2017) and surface elevation contours (light gray; Fretwell et al., 2013) and (c) bed roughness along profiles. (d) Magnitude of the bed elevation gradient derived from bed topography, with red showing a gradient of >80 m/km. (a–d) Marked are 15 m/yr ice flow speed isolines (black solid lines) for Bailey Ice Stream, Recovery, and Slessor Glaciers, including the northern tributary of Slessor Glacier (SN), the subglacial Recovery Lakes A–D (dashed black outlines) (Bell et al., 2007), the active subglacial lakes (white outlines) (Smith et al., 2009), the grounding line (dash-dotted line) (Rignot et al., 2013), the Shackleton Range and the Recovery-Slessor Gate (RSG).

of sediments and water (Rippin, Bamber, et al., 2006). Small subglacial lakes have been identified along the main trunk of Slessor Glacier (Smith et al., 2009). A 3 km thick sediment layer was identified in the Slessor catchment and hypothesized to influence ice dynamics (Bamber et al., 2006; Shepherd et al., 2006).

Here we present an improved bed topography map of the Recovery/Slessor/Bailey Region (Figure 1a), derived from new airborne radar data (Forsberg et al., 2017), filling a significant part of the data gap remaining in Bedmap2, the latest available Antarctic bedrock topography compilation (Fretwell et al., 2013). We use bed return power, elevation, and roughness along the radar profiles to infer controls on the location of fast ice flow tributaries and their potential to change.

2. Data and Methods

We use radar data (Ferraccioli et al., 2018) and existing data (Figure S1 in the supporting information) to derive a new bed topography map for the Recovery/Slessor/Bailey Region using kriging. Details about the processing and picking of the bed are given in the supporting information (Text S1).

Bed roughness following Rippin et al. (2014) was calculated along the radar profiles for 1.28 km windows and averaged over 5 km afterward to analyze the large-scale roughness of the region (Text S2). We show true roughness values on a logarithmic scale to emphasize the span of the 4 orders of magnitude over which they range.

Radar wave bed return power, with geometrical correction, depends primarily on bed roughness, bed properties, and attenuation within the ice. Bed return power can be used as a proxy for the basal conditions after correcting for attenuation. Attenuation depends on the length of the radar wave travel path and the attenuation rate, which mainly depends on ice temperature. It is difficult to estimate attenuation rate in our study region as ice temperature is poorly constrained here. Hence, we test different attenuation rates and discuss the variations in return power in connection with variations in ice thickness.

If basal conditions, roughness, and englacial temperatures are the same, the bed return power measured at various locations should theoretically have the same dependency on ice thickness. In reality, second-order effects, for example, impurities and temperature variations with depth, can alter the bed return power. For our analysis we assume that the attenuation rate does not change over small spatial distances of 10 km or less, equivalent to several ice thicknesses. Nevertheless, changes are possible across the shear margin, where we can expect an increase in temperature due to strain heating and a change in ice anisotropy due to a change in the stress regime. Matsuoka et al. (2009) showed that the contribution of ice anisotropy to the attenuation rate is presumably negligible. Strain heating would lead to an increase in ice temperature (Harrison et al., 1998) and thus an increase in attenuation. Hence, we would expect a decrease in bed return power. However, in our data we observe the opposite, an increase in bed return power at the shear margin. We therefore attribute significant changes in bed return power over short distances with similar ice thicknesses to be due to changes in basal conditions and/or bed roughness.

Changes in bed return power due to changes in basal conditions depend on the reflectivity R between ice and bed. The highest reflectivity is expected between ice and water, with −3.5 dB. Reflectivity is significantly smaller for a transition between ice and dry sediment/rock, with −19 to −8 dB (Peters et al., 2005; Reynolds, 2011). Hence, return power can vary by 4.5–15.5 dB from changes in basal properties alone. A similarly strong change in return power can be caused by a change in ice thickness of 200–600 m, when attenuation rate and basal properties remain constant (Matsuoka et al., 2012). This would, however, be visible in the bed elevation data.

To examine the controls for the present location of fast ice flow, we analyze whether the shear margin (i) coincides with a large gradient in bed elevation or (ii) coincides with a large gradient in bed return power. Using the bed elevation map, we calculate the magnitude of the bed elevation gradient at the center of the two neighboring grid points (2 km window) and compare it to the location of the 15 m/yr ice flow speed isoline. If they coincide, ice flow is regarded as topographically controlled. Otherwise, we analyze the bed return power and roughness to derive information on basal conditions, that is, whether the bed is likely to be frozen or thawed and whether the bed is smooth or rough, respectively. We interpret a smooth bed as consisting of sediments that have been smoothed by fast flow. If the bedrock is rough, we interpret it to be composed of either crystalline rocks or, alternatively, mixed sedimentary and crystalline rocks, as inferred in parts of West Antarctica (Bingham et al., 2017; Smith et al., 2013).

3. Results

3.1. Bed topography of Recovery Glacier

The most prominent feature revealed by the new bed topography map (Figure 1a; zoom Figure S2a) is a deep trough underlying Recovery Glacier, extending 800 km inland, and reaching a depth of up to 2,200 m below sea level (bsl) near the grounding line. This trough, hereafter termed the Recovery Trough, splits into two branches further upstream (840 km grid north, 40 km grid east) separated by a subglacial mountain range. A mountain, 940 m above sea level, about 1,500 m higher than its surrounding, is located at the southwest tip of Lake B (690 km grid north, 210 km grid east). The downstream part of Recovery Glacier is confined by the Shackleton Range, which extends about 440 km inland from the coast, that is, twice as far as previously known and inferred from outcrops. At the eastern end of the Shackleton Range is a steep-sided, flat-bottomed valley connecting Recovery with Slessor Glaciers, hereafter referred to as the Recovery-Slessor Gate (RSG).

The smoothest area (Figure 1c; zoom Figure S2b) is at the Recovery Lakes A and B. The Recovery Trough east of −300 km grid east is also remarkably smooth, with roughness values only 1 order of magnitude higher than for the Recovery Lakes. The RSG is similarly smooth. The mountains bounding the Recovery Trough west of −100 km grid east have the highest roughness values, with a distinct boundary between the smooth trough and the rough mountains of 2 orders of magnitude, corresponding to the 15 m/yr ice velocity isoline.

Fast ice flow of Recovery Glacier is topographically controlled between the grounding line and about −100 km grid east on the southern margin (Figure 1d; zoom Figure S2c). Along the northern margin, fast ice flow is topographically controlled between the grounding line and the RSG and beyond the RSG to −20 km grid east. Further east along the northern margin ice flow is not topographically controlled.

3.2. Bed Topography of Slessor Glacier and Bailey Ice Stream

The bed of Slessor Glacier is deep (Figure 1a; zoom Figure S2d) up to 1,670 m bsl in the upstream area of the northern tributary of Slessor Glacier (SN; 1,275 km grid north, −225 km grid east). Bailey Ice Stream, only a few kilometers away, is shallower than Slessor Glacier, only 1,500 m bsl at the grounding line. While Slessor Glacier reaches almost 600 km inland, with three major ice flow tributaries draining an area of 480,000 km^2, Bailey Ice Stream penetrates only 200 km inland and drains a relatively small area (80,000 km^2; Figure 1b). Notably, a deep trough (hereafter termed Bailey Trough) extends upstream from Bailey Ice Stream's current onset to connect directly to the onset of SN (Figure 1a; zoom Figure S1d). However, this topographic trough does not direct ice flow into Bailey Ice Stream; instead, ice from this region flows into Slessor Glacier, forming SN.

The smoothest bed (Figure 1c; zoom Figure S2e) is in the Bailey Trough, with similar roughness values as in the Recovery Trough. There is no change in roughness across the western 15 m/yr isoline of SN. Roughness increases along flow underneath SN from about 1,250 km grid north. This higher basal roughness is reflected in surface roughness, as seen in Moderate Resolution Imaging Spectroradiometer (MODIS) imagery (Haran et al., 2014).

Fast ice flow of Slessor Glacier is topographically controlled inland from the grounding line (Figure 1d; zoom Figure S2f). The eastern shear margin of SN and the low-speed area within SN (−390 km grid east, 1,160 km grid north) are topographically controlled but not the western shear margin of SN. Bailey Ice Stream is topographically controlled along its eastern margin. The bed elevation gradient is less pronounced along the western shear margin but still coincides with the 15 m/yr ice flow isoline. Hence, the location of the current fast ice flow of Bailey Ice Stream is topographically controlled.

4. Discussion

We use bed return power and bed roughness (Figure 1c) to examine glacier shear margins, which are not topographically controlled. Similar studies have been carried out for glaciers in West Antarctica, for example, at Thwaites Glacier (MacGregor et al., 2013; Schroeder et al., 2016), Institute and Möller Ice Streams (Bingham & Siegert, 2007b; Siegert et al., 2016), and the Siple Coast region (Catania et al., 2003; Raymond et al., 2006).

4.1. Fast Ice Flow of Recovery Glacier

We analyze one radar profile in detail crossing the 15 m/yr isoline (Figure 2a) to investigate controls other than topography on the location of fast ice flow in the upstream region of Recovery Glacier (east of −20 km grid east). Despite a small gradient in ice thickness of 6 m/km between 40 and 80 km distance along this radar profile, we observe an increase in bed return power (corrected for geometrical spreading) of about 3 dB and an increase in ice flow speed of 20 m/yr (Figure 2b). We tested likely attenuation rates for this region ranging from 4 to 10 dB/km (Langley et al., 2011; Matsuoka, 2011) and observe an increase in the corrected return power between 50 and 60 km, as indicated by the black arrow in Figure 2c. The return power averaged in the region of slow ice flow is 3–7 dB less than in the region of fast flowing ice (depending on the applied attenuation rate), a clear indication that the increase in ice flow speed is related to a change in basal conditions. If we had applied higher attenuation rates to correct for the small difference in ice thickness along the examined profile, the increase in bed return power corresponding to the increase in ice flow speed would become even more apparent. No clear change in roughness can be observed at the boundary of the 15 m/yr isoline (Figure 2a). Thus, we conclude that the step change in bed return power is unlikely due to a transition in bed conditions such as a change from sediment to crystalline rock. The observed return power increase can, however, be explained by the transition from dry to wet bed conditions, that is, by the presence of a thin water film or saturated sediments at the bed. Similar variable bed conditions have, for example, been observed at Rutford Ice Stream, where water plays an important role in the control of fast ice flow (Vaughan et al., 2008).

We conclude that the flow of the downstream region of Recovery Glacier (west of about −100 km grid east) is confined by topography and is therefore restricted in its location. The location of the fast flow tributaries in the upstream region is confined by the variability in basal conditions. Therefore, tributary migration is possible there if ice thickness and/or subglacial water flow change.

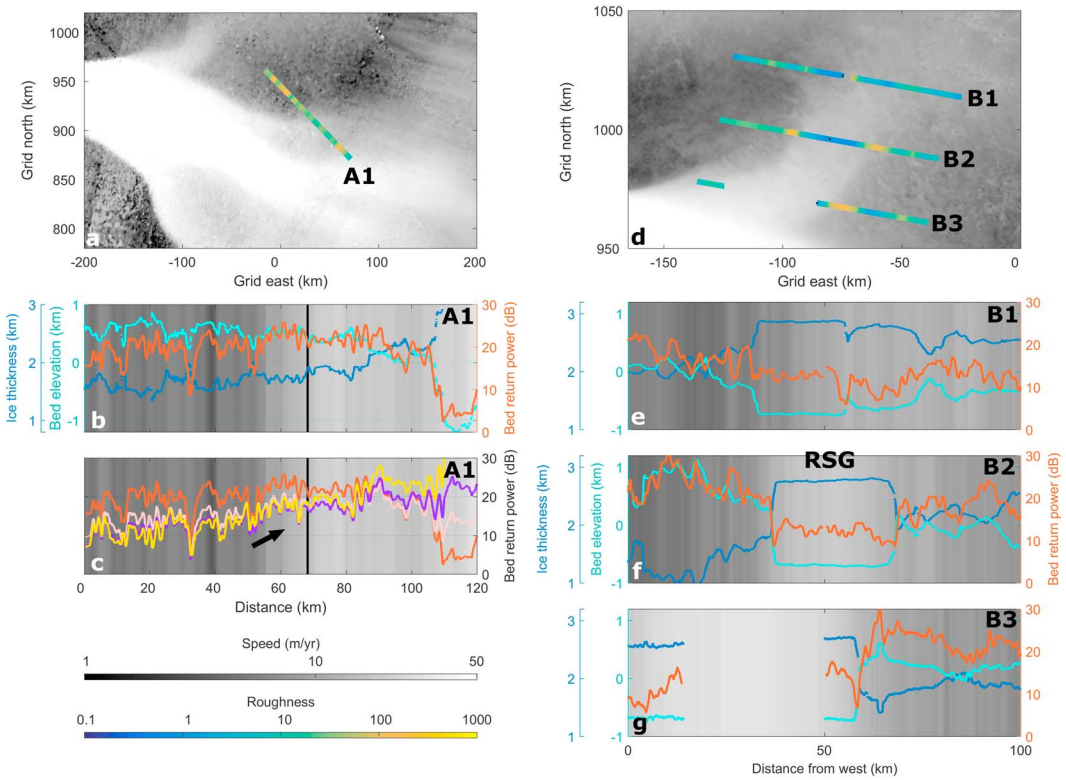

Figure 2. Basal conditions over topographic high at Recovery Glacier (a–c) and for the Recovery-Slessor Gate (RSG) (d–g). Ice flow velocity over topographic high at Recovery Glacier (a) and RSG (d) and the location of the radar profile A1 and B1–B3 shown in (b–c) and (e–g), respectively, colored with roughness values. (b and e–g) Bed elevation (cyan), ice thickness (blue), and relative bed return power (orange) along radar profiles. (c) Relative bed return power corrected for one-way attenuation rates of 0 (orange, same as in (b)), 4 (pink), 7 (purple), and 10 dB/km (yellow); the black arrow indicates the increase in return power between 50 and 60 km distance. Return power for all attenuation rates is corrected for geometric effects, relative to their respective minimum, and averaged over 1 km. Background color gives the ice flow speed (Mouginot et al., 2017) along these profiles (b and c, and e–g), black line the 15 m/yr ice flow speed (b and c).

4.2. Paleo–Ice Flow Through RSG

To evaluate the past variations in ice flow within the Recovery/Slessor/Bailey Region, we consider the RSG, the distinct topographic deepening at the eastern edge of the Shackleton Range (Figures 1a and 2d–2g). The surface elevation over the RSG decreases by about 2.7 m/km from Slessor Glacier to Recovery Glacier, with only slightly enhanced ice flow of about 20 m/yr (Figure 2d).

A decrease in bed return power can be observed together with an increase in ice thickness along the profiles B1–B3 crossing the RSG, as expected (Figures 2e–2g). For attenuation rate corrections between 4 and 7 dB/km, bed return power values within the RSG are similar to the values for the mountain areas on either side of the gate along profile B1 (Figure S3). A very smooth bed, as observed for the RSG (Figure 2d), can be an indication of water. However, as bed return power does not significantly increase within the RSG, we conclude that the RSG is very smooth but that no water is currently present at the bed.

We attribute the very smooth bed and well-defined trough to be due to formerly fast ice flow through the RSG. With ice flow from Slessor catchment to Recovery Glacier the RSG would have eroded over multiple glacial cycles. Additionally, observation of buckled englacial layers in the Slessor catchment area were interpreted as being caused by fast ice flow from Slessor Glacier to Recovery Glacier, as recently as the Last Glacial Maximum (LGM) (Rippin, Siegert, et al., 2006).

4.3. Fast Ice Flow of Bailey Ice Stream and Slessor Glacier

The western shear margin of SN underlain by Bailey Trough (Figure 3) is not topographically controlled. We analyze radar profiles crossing this shear margin to elucidate controls on ice flow directions of Bailey Ice Stream

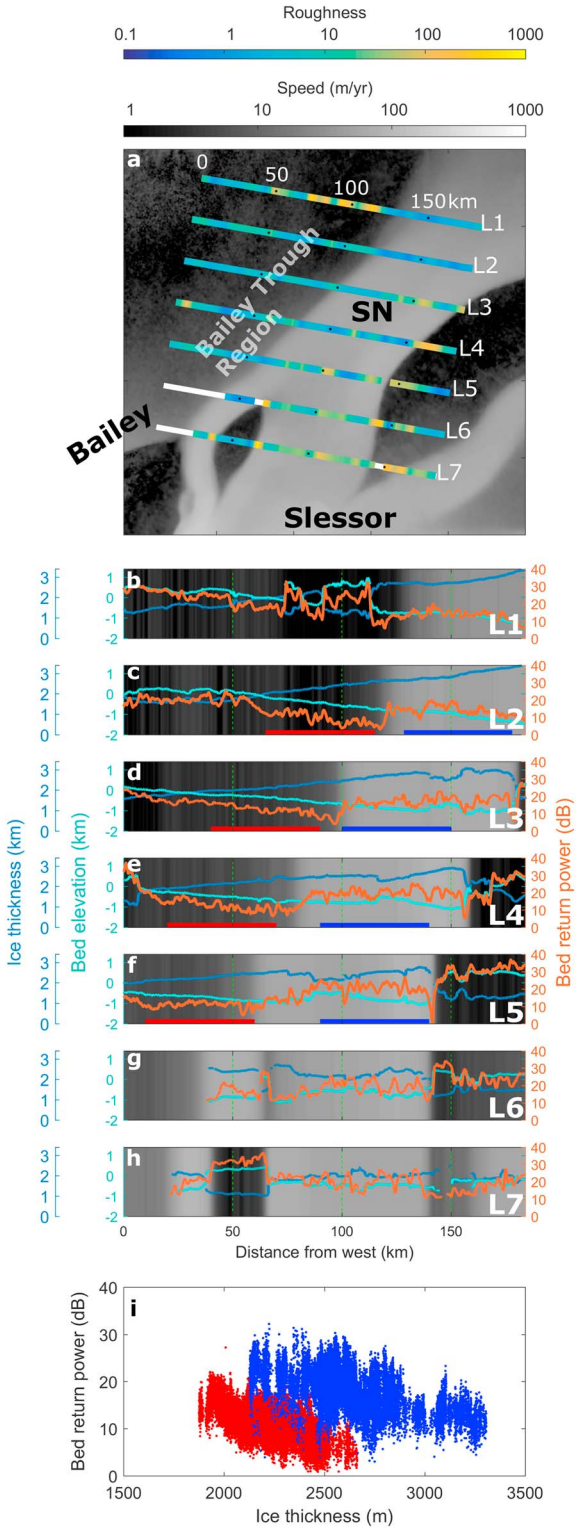

Figure 3. Bed topography and subglacial hydrology revealed by radar data. (a) Radar profile locations (L1–L7) with bed roughness (color along profiles) crossing the Bailey Trough Region and northern tributary of Slessor Glacier (SN). (b–h) Bed elevation (cyan), ice thickness (blue), and relative bed return power (orange) along profiles L1–L7. Background color gives the ice flow speed (Mouginot et al., 2017) along these profiles. The relative bed return power (orange) was corrected for geometric effects and averaged over 1 km but not corrected for attenuation. (i) Geometrically corrected bed return power plotted against thickness for 50 km long segments of profiles L2–L5 (marked in (c–f) with red and blue bars) for the Bailey Trough Region (red) and Slessor Glacier (blue).

and Slessor Glacier. Hereafter, we will refer to the region upstream of Bailey Ice Stream and west of the western shear margin of SN as the Bailey Trough Region (Figure 3a).

Bed elevation decreases over the shear margin from the Bailey Trough Region to SN (profiles L2–L5; Figures 3c–3f), and a significant increase in bed return power can be observed along profiles L2 (at 120 km), L3 (at 100 km), L4 (at 80 km), and L5 (at 60 km). This increase becomes even more apparent for attenuation rate corrections between 4 and 10 dB/km (Figure S4). The larger the attenuation rate, the higher is the increase in return power from the Bailey Trough Region to SN. If we assume an increase in attenuation rate due to strain heating across this shear margin, we would expect a decrease in bed return power, as observed at Institute Ice Stream (Siegert et al., 2016). However, we observe the opposite, an increase in bed return power over this shear margin.

Figure 3i shows bed return power plotted over ice thickness for the Bailey Trough Region (red) and SN (blue). As expected, we observe a clear dependency of bed return power on ice thickness in both areas. However, the bed return power, for a given ice thickness, is higher for SN than for the Bailey Trough Region. As we assume no strong variations in attenuation rate between these neighboring areas, we interpret this difference (Figure 3i) to be caused by changes in the basal properties.

From radar profiles crossing the Bailey Trough Region and SN we derive an approximate regional attenuation rate of 7 ± 4.5 dB/km (Figure 3i). From this we calculate the difference in bed reflectivity between SN and the Bailey Trough Region to be between 12 and 14 dB. These values fit within the range in reflectivity difference expected between an ice to water/sediment boundary and an ice to water boundary (section 2), indicating that the bed of the Bailey Trough Region is dry, while water influences the fast ice flow of SN.

We observe an increase in roughness from the northern profiles to the southern profiles (Figure 3a). The bed is smooth along the radar profiles crossing the area of high flow speeds at the onset of SN (L1 and L2; mean roughness of 2) and west of SN in the Bailey Trough Region (mean roughness of 7 for L4). Further downstream, the basal roughness increases to 25 along L5 and 33 along L7, a significant increase in an area expected to be smoothed by fast ice flow. Increased bed roughness is also reflected in rougher ice surface (Figures 1c and S2f). A rough bed has also been observed at Pine Island Glacier, where seismic data showed that crystalline bedrock is overlain by up to 10 m of sediments (Bingham et al., 2017; Brisbourne et al., 2017). However, such information cannot be derived from our radar data alone. Therefore, we conclude that the very rough bed under Slessor Glacier is likely crystalline bedrock, since a sedimentary bed should have been smoothed by fast ice flow. The smoother bed observed beneath the Bailey Trough Region is reminiscent of the smooth sedimentary bed previously observed beneath the onset of SN (Shepherd et al., 2006).

Variations in bed return power are 10 dB larger for Slessor Glacier than for the Bailey Trough Region (Figures 3c–3f). While variations in bed return power coincide at some locations with variations in bed elevation, these bed return power variations are significantly larger than can be explained by ice thickness differences of only 100–200 m. Hence, we interpret these large bed return power variations for Slessor Glacier as being due to mixed bed conditions, that is, alternating patches of wet and dry crystalline bed.

We conclude that fast ice flow of SN is determined by the presence of water at the bed, controlling the location of the boundary to the neighboring Bailey Trough Region. The bed of the Bailey Trough Region consists of dry sediments.

4.4. Changes of Fast Ice Flow in the Recovery/Slessor/Bailey Region

The RSG between the Slessor catchment and Recovery Glacier is inferred to have been incised by fast ice flow in the past. To generate the necessary ice flow speeds to erode this gate, the surface gradient over the RSG must have been higher in the past. This is possible if the Recovery Glacier surface was lower than present and/or the surface in the Slessor catchment area was higher. Studies of the paleo–ice streams suggest that ice elevation changes have occurred here during the carving of the deep troughs, between the Oligocene and Mid-Miocene (Paxman et al., 2017; Sugden et al., 2014). At the same time no significant differences in ice thickness for Recovery and Slessor Glaciers could be found for the LGM compared to present conditions (Hein et al., 2011). However, englacial layer studies (Rippin, Siegert, et al., 2006) suggest that the RSG connection was active as recently as the LGM, showing that dynamic changes in the region have occurred since then.

Bamber et al. (2006) concluded from a survey in the Slessor catchment area that the onset of SN is likely underlain by a thick layer of marine sediments. Based on the smooth bed we observe in the region, we conclude that sediments are likely under the Bailey Trough Region and at the onset of SN. However, the rough

bed below Slessor Glacier in the region of fastest ice flow and along parts of SN shows that a crystalline bed is more likely here. This is in agreement with basal shear stress values in this region, as modeled by Joughin et al. (2006). Larger shear stresses are an indication of a more rigid bed, while low shear stresses indicate a softer bed, which is easier to deform. Joughin et al. (2006) infer a weak bed at the grounding line of Slessor Glacier, indicating possible lubricated sediments, and significantly higher basal shear stress further upstream, indicating crystalline bed.

The Bailey Trough with its smooth sedimentary bed continues into the upstream area of SN. Current ice flow from the catchment of SN is controlled by the location of water. Hence, there is potential of change in the direction of fast ice flow from SN to Bailey Ice Stream. Both the bed and surface topography (Figures 1a and 1c) suggest that fast ice flow from the onset of SN might have been along Bailey Ice Stream in the past, while at present SN flows into the main Slessor Glacier trunk over a rough bed that presumably used to separate a larger Bailey Ice Stream from Slessor Glacier.

Observations of englacial layers at the Korff Ice Rise downstream from Institute Ice Stream show that dynamic changes have occurred here in the past (Kingslake et al., 2016). A model study of the West Antarctica ice streams draining into the Filchner-Ronne Ice Shelf shows that the Institute and Möller Ice Streams are highly sensitive to basal melting (Wright et al., 2014). Our data suggest past ice piracy from Bailey Ice Stream to Slessor Glacier and from Slessor Glacier to Recovery Glacier through the RSG, showing that the Recovery/Slessor/Bailey Region has also undergone major dynamic changes in the past, with changes of the relative ice fluxes though its three main glaciers.

Flow lines (Figure S5) show that the bed of Slessor Glacier is significantly deeper than the bed of Bailey Ice Stream inland of the grounding line. The grounding lines for Slessor Glacier and Bailey Ice Stream are currently on the edge toward a retrograde bed, suggesting an unstable grounding line position, the possibility of warm water infiltration, with subsequent grounding line retreat. The bed elevation of Bailey Ice Stream from the grounding line decreases by 650 m, followed by a gentle prograde slope. In contrast, Slessor Glacier shows a decrease in bed elevation by 1,100 m, followed by a steep increase, reaching a plateau afterward. This suggests differences in the sensitivity of these two glaciers to the penetration of warm ocean waters into the ice shelf cavity by the end of the century, as predicted by Hellmer et al. (2012). Further, it indicates that a large reorganization of ice flux from the Recovery/Slessor/Bailey Region to the Filchner Ice Shelf is possible, once the retreat of the grounding lines is initiated.

5. Conclusions

We identify different controls for the location of fast ice flow in the Recovery/Slessor/Bailey Region, the largest potential contributor to long-term future sea level rise from East Antarctica (Golledge et al., 2017). Recovery Glacier is topographically controlled in its downstream area. Hence, the location of fast flow is unlikely to change there. Further upstream, however, the shear margin is less controlled by topography, and basal water plays a key role in facilitating enhanced flow. Therefore, the probability is greater for fast ice flow to change its position in the upstream area. A topographic gate connects the Slessor catchments with Recovery Glacier, through which ice was likely steered in the past, potentially as recently as the LGM (Rippin, Siegert, et al., 2006). A similar connectivity could reoccur in future, driven by ice sheet surface elevation changes.

Slessor Glacier is underlain by a deeper trough than Bailey Ice Stream, in particular, at the grounding line. Notably, most of the present fast ice flow is focused along the tributaries of Slessor Glacier. The location and width of SN are controlled by subglacial water, leading to a clear boundary to the adjacent Bailey Trough. However, former ice flow from SN likely fed directly into Bailey Ice Stream.

Overall, several fast ice flow tributaries of Recovery Glacier, Slessor Glacier, and Bailey Ice Stream appear to have changed in the past, likely triggered by changes in ice sheet thickness or basal water routing. We conclude that similar changes could potentially reoccur in the future in this key sector of East Antarctica.

Acknowledgments
The ICEGRAV Antarctic airborne survey was flown in 2013 and was sponsored by the U.S. National Geospatial-Intelligence Agency, DTU Space (Denmark), and the Center for Ice, Climate and Ecosystems (ICE) for the Norwegian Polar Institute (NPI), with significant logistics and in-kind contributions by the British Antarctic Survey (BAS), NPI, and the Instituto Antártico Argentino. BAS flew the survey with its aerogeophysical survey platform, a Twin Otter. The Antarctic Logistics Center International (ALCI) prepared fuel at FD83 that was used for the NPI-led field camp at Recovery Lakes. We especially thank M. Ghidella and A. Zakrajsek (Instituto Antárctico Argentino) for their field campaign support. Postfield activities at NPI are supported by the Research Council of Norway's FRINATEK program (project: 240944). F. F. and T. J. acknowledge financial support from the BAS Geology and Geophysics team/grant (bas0100029) of the Polar Science for Planet Earth program. We thank Egidio Armadillo, Robert Bingham, and the anonymous reviewer for their comments, which greatly helped to improve the manuscript. The processed ICEGRAV radar data are freely available on the NERC/BAS Polar Data Centre airborne geophysics data portal (https://doi.org/10.5285/6549203d-da8b-4a22-924b-a9e1471ea7f1).

References

Bamber, J. L., Ferraccioli, F., Joughin, I., Shepherd, T., Rippin, D. M., Siegert, M. J., et al. (2006). East Antarctic ice stream tributary underlain by major sedimentary basin. *Geology*, *34*(1), 33–36. https://doi.org/10.1130/G22160.1

Bell, R. E., Studinger, M., Shuman, C. A., Fahnestock, M. A., & Joughin, I. (2007). Large subglacial lakes in East Antarctica at the onset of fast-flowing ice streams. *Nature*, *445*, 904–907. https://doi.org/10.1038/nature05554

Bingham, R. G., & Siegert, M. J. (2007a). Radar-derived bed roughness characterization of Institute and Möller ice streams, West Antarctica, and comparison with Siple Coast ice streams. *Geophysical Research Letters*, *34*, L21504. https://doi.org/10.1029/2007GL031483
Bingham, R. G., & Siegert, M. J. (2007b). Radio-echo sounding over polar ice masses. *Journal of Environmental and Engineering Geophysics*, *12*(1), 47–62.
Bingham, R. G., Vaughan, D. G., King, E. C., Davies, D., Cornford, S. L., Smith, A. M., et al. (2017). Diverse landscapes beneath Pine Island Glacier influence ice flow. *Nature Communications*, *8*(1), 1618. https://doi.org/10.1038/s41467-017-01597-y
Brisbourne, A. M., Smith, A. M., Vaughan, D. G., King, E. C., Davies, D., Bingham, R. G., et al. (2017). Bed conditions of Pine Island Glacier, West Antarctica. *Journal of Geophysical Research: Earth Surface*, *122*, 419–433. https://doi.org/10.1002/2016JF004033
Catania, G. A., Conway, H. B., Gades, A. M., Raymond, C. F., & Engelhardt, H. (2003). Bed reflectivity beneath inactive ice streams in West Antarctica. *Annals of Glaciology*, *36*, 287–291. https://doi.org/10.3189/172756403781816310
Ferraccioli, F., Corr, H., Jordan, T., Forsberg, R., Matsuoka, K., Diez, A., et al. (2018). Bed, surface elevation and ice thickness measurements derived from Radar acquired during the ICEGRAV-2013 airborne geophysics campaign, Polar Data Centre, British Antarctic Survey NERC, Cambridge, UK. https://doi.org/10.5285/6549203d-da8b-4a22-924b-a9e1471ea7f1
Forsberg, R., Olesen, A. V., Ferraccioli, F., Jordan, T. A., Matsuoka, K., Zakrajsek, A., et al. (2017). Exploring the Recovery Lakes region and interior Dronning Maud Land, East Antarctica, with airborne gravity, magnetic and radar measurements. *Geological Society of London, Special Publications*, *461*, 23–34. https://doi.org/10.1144/SP461.17
Fretwell, P., Pritchard, H. D., Vaughan, D. G., Bamber, J. L., Barrand, N. E., Bell, R., et al. (2013). Bedmap2: Improved ice bed, surface and thickness datasets for Antarctica. *The Cryosphere*, *7*(1), 375–393. https://doi.org/10.5194/tc-7-375-2013
Fricker, H. A., Carter, S. P., Bell, R. E., & Scambos, T. (2014). Active lakes of Recovery Ice Stream, East Antarctica: A bedrock-controlled subglacial hydrological system. *Journal of Glaciology*, *60*(223), 1015–1030. https://doi.org/10.3189/2014JoG14J063
Golledge, N. R., Levy, R. H., McKay, R. M., & Naish, T. R. (2017). East Antarctic ice sheet most vulnerable to Weddell Sea warming. *Geophysical Research Letters*, *44*, 2343–2351. https://doi.org/10.1002/2016GL072422
Haran, T., Bohlander, J., Scambos, T., Painter, T., & Fahnestock, M. (2014). MODIS Mosaic of Antarctica 2008–2009 (MOA2009) Image Map.
Harrison, W. D., Echelmeyer, K. A., & Larsen, C. F. (1998). Measurement of temperature in a margin of Ice Stream B, Antarctica: Implications for margin migration and lateral drag. *Journal of Glaciology*, *44*(148), 615–624. https://doi.org/10.3189/S0022143000002112
Hein, A. S., Fogwill, C. J., Sugden, D. E., & Xu, S. (2011). Glacial/interglacial ice-stream stability in the Weddell Sea embayment, Antarctica. *Earth and Planetary Science Letters*, *307*(1–2), 211–221. https://doi.org/10.1016/j.epsl.2011.04.037
Hellmer, H. H., Kauker, F., Timmermann, R., Determann, J., & Rae, J. (2012). Twenty-first-century warming of a large Antarctic ice-shelf cavity by a redirected coastal current. *Nature*, *485*, 225–228. https://doi.org/10.1038/nature11064
Jordan, T. A., Ferraccioli, F., Ross, N., Corr, H. F., Leat, P. T., Bingham, R. G., et al. (2013). Inland extent of the Weddell Sea Rift imaged by new aerogeophysical data. *Tectonophysics*, *585*, 137–160. https://doi.org/10.1016/j.tecto.2012.09.010
Joughin, I., Bamber, J. L., Scambos, T., Tulaczyk, S., Fahnestock, M., & MacAyeal, D. R. (2006). Integrating satellite observations with modelling: Basal shear stress of the Filcher-Ronne ice streams, Antarctica. *Philosophical Transactions of the Royal Society of London A: Mathematical, Physical and Engineering Sciences*, *364*(1844), 1795–1814. https://doi.org/10.1098/rsta.2006.1799
Kingslake, J., Martín, C., Arthern, R. J., Corr, H. F. J., & King, E. C. (2016). Ice-flow reorganization in West Antarctica 2.5 kyr ago dated using radar-derived englacial flow velocities. *Geophysical Research Letters*, *43*, 9103–9112. https://doi.org/10.1002/2016GL070278
Langley, K., Kohler, J., Matsuoka, K., Sinisalo, A., Scambos, T., Neumann, T., et al. (2011). Recovery Lakes, East Antarctica: Radar assessment of sub-glacial water extent. *Geophysical Research Letters*, *38*, L05501. https://doi.org/10.1029/2010GL046094
Le Brocq, A. M., Hubbard, A., Bentley, M. J., & Bamber, J. L. (2008). Subglacial topography inferred from ice surface terrain analysis reveals a large un-surveyed basin below sea level in East Antarctica. *Geophysical Research Letters*, *35*, L16503. https://doi.org/10.1029/2008GL034728
MacGregor, J. A., Catania, G. A., Conway, H., Schroeder, D. M., Joughin, I., Young, D. A., et al. (2013). Weak bed control of the eastern shear margin of Thwaites Glacier, West Antarctica. *Journal of Glaciology*, *59*(217), 900–912. https://doi.org/10.3189/2013JoG13J050
Matsuoka, K. (2011). Pitfalls in radar diagnosis of ice-sheet bed conditions: Lessons from englacial attenuation models. *Geophysical Research Letters*, *38*, L05505. https://doi.org/10.1029/2010GL046205
Matsuoka, K., MacGregor, J. A., & Pattyn, F. (2012). Predicting radar attenuation within the Antarctic ice sheet. *Earth and Planetary Science Letters*, *359–360*, 173–183. https://doi.org/10.1016/j.epsl.2012.10.018
Matsuoka, K., Wilen, L., Huerly, S. P., & Raymond, C. F. (2009). Effects of birefringence within ice sheets on obliquely propagating radio waves. *IEEE Transactions on Geoscience and Remote Sensing*, *47*(5), 1429–1443.
Mouginot, J., Rignot, E., Scheuchl, B., & Millan, R. (2017). Comprehensive annual ice sheet velocity mapping using Landsat-8, Sentinel-1, and Radarsat-2 data. *Remote Sensing*, *9*, 364. https://doi.org/10.3390/rs9040364
Paxman, G. J. G., Jamieson, S. S. R., Ferraccioli, F., Bentley, M. J., Forsberg, R., Ross, N., et al. (2017). Uplift and tilting of the Shackleton Range in East Antarctica driven by glacial erosion and normal faulting. *Journal of Geophysical Research: Solid Earth*, *122*, 2390–2408. https://doi.org/10.1002/2016JB013841
Peters, M. E., Blankenship, D. D., & Morse, D. L. (2005). Analysis techniques for coherent airborne radar sounding: Application to West Antarctic ice streams. *Journal of Geophysical Research*, *110*, B06303. https://doi.org/10.1029/2004JB003222
Raymond, C., Catania, G. A., Nereson, N., & Van Der Veen, C. (2006). Bed radar reflectivity across the north margin of Whillans Ice Stream, West Antarctica, and implications for margin processes. *Journal of Glaciology*, *52*(176), 3–10. https://doi.org/10.3189/172756506781828890
Reynolds, J. M. (2011). *An introduction to applied and environmental geophysics* (2nd ed.). Oxford: Wiley-Blackwell.
Rignot, E., Bamber, J. L., van den Broeke, M. R., Davis, C., Li, Y., van de Berg, W. J., et al. (2008). *Recent Antarctic ice mass loss from radar interferometry and regional climate modelling*, *1*, 106–110. https://doi.org/10.1038/ngeo102
Rignot, E., Jacobs, S., Mouginot, J., & Scheuchl, B. (2013). Ice-shelf melting around Antarctica. *Science*, *341*(6143), 266–270. https://doi.org/10.1126/science.1235798
Rignot, E., Mouginot, J., & Scheuchl, B. (2011). Ice flow of the Antarctic ice sheet. *Science*, *333*(6048), 1427–1430. https://doi.org/10.1126/science.1208336
Rippin, D., Bamber, J., Siegert, M., Vaughan, D., & Corr, H. (2006). Basal conditions beneath enhanced-flow tributaries of Slessor Glacier, East Antarctica. *Journal of Glaciology*, *52*(179), 481–490. https://doi.org/10.3189/172756506781828467
Rippin, D., Bingham, R., Jordan, T., Wright, A., Ross, N., Corr, H., et al. (2014). Basal roughness of the Institute and Möller Ice Streams, West Antarctica: Process determination and landscape interpretation. *Geomorphology*, *214*, 139–147. https://doi.org/10.1016/j.geomorph.2014.01.021
Rippin, D. M., Bamber, J. L., Siegert, M. J., Vaughan, D. G., & Corr, H. F. J. (2003). Basal topography and ice flow in the Bailey/Slessor region of East Antarctica. *Journal of Geophysical Research*, *108*(F1), 6008. https://doi.org/10.1029/2003JF000039

Rippin, D. M., Bamber, J. L., Siegert, M. J., Vaughan, D. G., & Corr, H. F. J. (2004). The role of ice thickness and bed properties on the dynamics of the enhanced-flow tributaries of Bailey Ice Stream and Slessor Glacier, East Antarctica. *Annals of Glaciology*, *39*(1), 366–372. https://doi.org/10.3189/172756404781814375

Rippin, D. M., Siegert, M. J., Bamber, J. L., Vaughan, D. G., & Corr, H. F. J. (2006). Switch-off of a major enhanced ice flow unit in East Antarctica. *Geophysical Research Letters*, *33*, l15501. https://doi.org/10.1029/2006GL026648

Schroeder, D. M., Grima, C., & Blankenship, D. D. (2016). Evidence for variable grounding-zone and shear-margin basal conditions across Thwaites Glacier, West Antarctica. *Geophysics*, *81*(1), WA35–WA43. https://doi.org/10.1190/geo2015-0122.1

Shepherd, T., Bamber, J., & Ferraccioli, F. (2006). Subglacial geology in Coats Land, East Antarctica, revealed by airborne magnetics and radar sounding. *Earth and Planetary Science Letters*, *244*(1), 323–335. https://doi.org/10.1016/j.epsl.2006.01.068

Siegert, M. J., Ross, N., Li, J., Schroeder, D. M., Rippin, D., Ashmore, D., et al. (2016). Subglacial controls on the flow of Institute Ice Stream, West Antarctica. *Annals of Glaciology*, *57*(73), 19–24. https://doi.org/10.1017/aog.2016.17

Smith, A. M., Jordan, T. A., Ferraccioli, F., & Bingham, R. G. (2013). Influence of subglacial conditions on ice stream dynamics: Seismic and potential field data from Pine Island Glacier, West Antarctica. *Journal of Geophysical Research: Solid Earth*, *118*, 1471–1482. https://doi.org/10.1029/2012JB009582

Smith, B. E., Fricker, H. A., Joughin, I. R., & Tulaczyk, S. (2009). An inventory of active subglacial lakes in Antarctica detected by ICESat (2003–2008). *Journal of Glaciology*, *55*(192), 573–595. https://doi.org/10.3189/002214309789470879

Sugden, D., Fogwill, C., Hein, A., Stuart, F., Kerr, A., & Kubik, P. (2014). Emergence of the Shackleton Range from beneath the Antarctic Ice Sheet due to glacial erosion. *Geomorphology*, *208*, 190–199. https://doi.org/10.1016/j.geomorph.2013.12.004

Vaughan, D. G., Corr, H. F., Smith, A. M., Pritchard, H. D., & Shepherd, A. (2008). Flow-switching and water piracy between Rutford Ice Stream and Carlson Inlet, West Antarctica. *Journal of Glaciology*, *54*(184), 41–48. https://doi.org/10.3189/002214308784409125

Winsborrow, M. C., Clark, C. D., & Stokes, C. R. (2010). What controls the location of ice streams? *Earth-Science Reviews*, *103*(1–2), 45–59. https://doi.org/10.1016/j.earscirev.2010.07.003

Wright, A. P., Le Brocq, A. M., Cornford, S. L., Bingham, R. G., Corr, H. F. J., Ferraccioli, F., et al. (2014). Sensitivity of the Weddell Sea sector ice streams to sub-shelf melting and surface accumulation. *The Cryosphere*, *8*(6), 2119–2134. https://doi.org/10.5194/tc-8-2119-2014